A Thesis

entitled

A Study of Control Systems for Brushless DC Motors

by

Omar Mohammed

Submitted to the Graduate Faculty as partial fulfillment of the requirements for the

Master of Science Degree in Electrical Engineering

_____

Dr. Thomas Stuart, Committee Chair

_____

Dr. Mansoor Alam, Committee Member

_____

Dr. Richard Molyet, Committee Member

_____

Dr. Patricia R. Komuniecki, Dean
College of Graduate Studies

The University of Toledo

August 2014

An Abstract of

A Study of Control Systems for Brushless DC Motors

by

Omar Mohammed

Submitted to the Graduate Faculty as partial fulfillment of the requirements for the Master of Science Degree in Electrical Engineering

The University of Toledo

August 2014

Brushless DC (BLDC) are replacing DC motors in wide range of applications such as household appliances, automotive and aviation. These applications require a very robust, high power density and efficient motor for operation. BLDCs are commutated electronically unlike the DC motor. BLDCs are controlled using a microcontroller which powers a three phase power semiconductor bridge. This semiconductor bridge provides power to the stator windings based on the control algorithm. The motor is electronically commutated, and the control technique/ algorithm required for commutation can be achieved either by using a sensor or a sensorless approach. To achieve the desired level of performance the motor also can be controlled using a velocity feedback loop.

Sensorless control techniques such as Direct Back Electromotive Force (Back-EMF), Indirect Back EMF Integration and Field Oriented Control (FOC) are studied and discussed.

To achieve a desired level of performance in various applications that require the motor to operate at constant speed over various loads, the motor has to be operated using a suitable velocity control loop. These types of controllers are achieved by using a conventional proportional- integral (PI) controller.

The speed vs. torque characteristics of several different sensorless control techniques of BLDCs were studied and compared to the speed vs. torque curve of a separately excited DC motor. The speed vs. torque characteristic of a BLDC using a PI controller is also discussed.

To my parents, family and friends

Acknowledgements

I sincerely thank Dr. Thomas Stuart for providing guidance towards my research. It has been a great learning experience working with him. I would like to express my deepest gratitude towards him for offering instructive advice at all times.

I also would like to thank Delphi of Kokomo, IN and Electronic Concepts and Engineering of Holland, OH for providing the Texas Instruments and Freescale evaluation kits for my research.

Last, but not least. I would like to thank my parents, family, and friends for their support throughout my graduate school journey.

Table of Contents

Abstract iii

Acknowledgements v

Table of Contents vi

List of Figures ix

List of Abbreviations xi

1. **Introduction 1**

1.1 BLDC motor applications 1

1.1.1 Open Loop Applications 1

1.1.2 Applications with speed control 2

1.1.3 Application with positioning applications 2

1.2 BLDCs vs. Conventional DC motors 2

1.3 A brief review on control of the BLDC motor 3

1.4 Problem Statement 4

1.5 Thesis Organization 4

2. **Overview of BLDC Design and Control 6**

2.1 BLDC Motor Construction 6

2.2. Architecture of the BLDC system 8

3. **Control Theory** **12**

3.1 Hall Effect sensors 13

3.2 Direct Back- EMF Zero Crossing Technique (Terminal Voltage Sensing/ Trapezoidal Control) 14

3.3 Indirect Back EMF Integration Technique 17

3.4 Field Oriented Control 19

3.3.1 Rotating Reference Frame 21

3.3.2 Space Vector Definition and Projection 22

3.3.2.1 The (a,b,c) → (α,β) Projection (Clarke Transformation) 22

3.3.2.2 The (α,β) → (d,q) Projection (Park Transformation) 23

3.3.3 Rotor flux position 23

4. **Speed- Torque Relationship of the BLDC** **25**

4.1 Torque- Speed characteristics 25

4.2 Velocity Control Using a PI Controller in a BLDC Drive: 30

4.2.1 Tuning the $\boldsymbol{Kp}$ and $\boldsymbol{Ki}$ gains: **30**

5. **Experimental Results** **33**

5.1 Prony Brake Dynamometer 33

5.2 Test Results of Speed vs. Torque for Different BLDC Control Techniques 35

5.2.1 TI Kit- DRV8312- 69M 36

5.2.2 Freescale- 3PhaseLV 38

6. **Conclusion and Future Work** **42**

6.1 Conclusion 42

6.2 Future Work 43

References 45
A BLDC KIT 47

List of Figures

2- 1: Outer and Inner Rotor Design of BLDC 7

2- 2: Block Diagram of BLDC Control 9

2- 3: Internal Block Diagram of the Power Converter and Controller 10

3- 1: Position of Hall Effect Sensors.....13

3- 2: Alignment of Phase Back EMF and Current.....15

3- 3: Three Phase Inverter and BLDC 16

3- 4: Integrated Area of the Back EMF for Different Speeds.....18

3- 5: Rotor and Stator 90 Degree Position in the BLDC 20

3- 6: Rotating Frame Representation of the d and q Axes.....21

3- 7: Two Axis Coordinate System.....22

3- 8: Internal Block Diagram of FOC.....23

4- 1: Speed vs. Torque of BLDC [16].....26

4- 2: Separately Excited DC Motor 27

4- 3: Speed vs. Torque of a Separately Excited DC Motor 28

4- 4: Block Diagram of a PI Controller 29

4- 5: Block Diagram of a Velocity Control Loop for a BLDC with PI Control.....30

4- 6: Closed Velocity Control Loop using PI in BLDC.....31

5-1: Prony Brake Dynamometer 34

5- 2: Prony Brake Setup 35

5-3: Speed vs. Torque of Trapezoidal BLDC Control by TI 36

5-4: Speed vs. Torque of the Direct Back EMF Using Hall Effect Sensors by TI 37

5-5: Speeds vs. Torque of Indirect Back EMF by TI 37

5-6: Speed vs. Torque of FOC by TI 38

5-7: Speed vs. Torque of Indirect Back EMF by Freescale 39

5-8: Speed vs. Torque of the Direct Back EMF by Freescale 39

5-9: Speed vs. Torque of Velocity Control Loop Using FOC 41

5-10: Speed vs. Torque of Velocity Control Loop Using Indirect Back EMF 41

A-1: DRV8312-69M kit by TI 48

A-2: F2806x Microcontroller Card (32 bit) 48

A-3**:** 3 Phase LV kit by Freescale 49

A-4: Freescale- MC9S08MP16 Control Card (8 bit) 50

A-5: Freescale- MC56F8006 Control Card (32 bit) 50

List of Abbreviations

ADC .....Analog to Digital Converter

Back- EMF .....Back Electromagnetic Force
BLDC .....Brushless DC Motor

DC .....Direct Current
DSC .....Digital Signal Controller

FOC .....Field Oriented Control

GUI .....Graphical User Interface

I/O .....Input/ Output

PMSM .....Permanent Magnet Synchronous Motor
PI Controller.....Proportional Integral Controller
PWM .....Pulse Width Modulation

RPM .....Revolutions Per Minute

SVM .....Space Vector Modulation

Chapter 1

Introduction

Household appliances are one of the fastest growing markets for BLDCs[1]. Common household appliances which use electric motors include air conditioners, refrigerators, vacuum cleaners, washers and dryers. These appliances have relied on traditional electric motors such as single phase AC motors including capacitor- start, capacitor- run motors, and universal motors. However, consumers now demand better performance, reduced acoustic noise and higher efficient motor for their appliances. Hence, BLDC have been introduced in order to fulfill these requirements.

Brushless DC motors (BLDC) are usually small horsepower control motors that provide various advantages such as high efficiency, quiet operation, high reliability, compact form and low maintenance. However, there are disadvantages for the BLDC because of variable speed, and therefore adjustable speed drives are used to overcome this.

1.1 BLDC motor applications

1.1.1 Open Loop Applications

Some examples representing open loop control are fans, pumps and blowers. These applications only require a simple low cost controller[1].

1.1.2 Applications with speed control

These applications may demand high speed control accuracy and good dynamic response. Some examples for these applications are washers, dryers and other household appliances. Applications with speed control are also found in the automotive area for uses such as fuel pumps, electronic steering, and engine controls. An advanced control algorithm is often required by these applications, which makes them more expensive [1].

1.1.3 Application with positioning applications

In these applications importance is given to fast dynamic response to speed and torque changes. Many industrial and automation applications come under this category. Also, some of these applications may have frequent reversals of rotational direction. A typical cycle in these applications will consist of four phases: an accelerating phase, a constant speed phase, a deceleration phase and a positioning phase[1]. The load on the motor can vary in all these phases, causing an increase in the complexity of the controller's algorithm. These systems mostly operate in closed loop with three control loops functioning simultaneously: a Torque Control Loop, a Speed Control Loop and a Position Control Loop[1]. Sometimes sensors are required to reduce the commutation time.

1.2 BLDCs vs. Conventional DC motors

In a conventional (brushed) DC motor, the brushes are responsible for making the mechanical contact with a set of electrical contacts on the rotor referred to as the commutator [1]. This forms an electric circuit between the DC electrical source and the armature coil windings. As the armature rotates, the stationary brushes come in contact

with different sections of the commutator. The rotating commutator and the brush- system form a set of electrical switches which operate in a sequence to allow electric current to flow through the armature coils closest to the field which may be an electromagnet or a permanent magnet [1].

In a BLDC motor, armature coils do not move, and instead, the permanent magnets rotate. Therefore the armature remains static which avoids the problem of how to transfer current to a moving armature [1]. In a BLDC the commutator assembly is replaced by an electronic controller which is programmed to perform the coil switching.

Listed below are some of the major advantages of BLDCs:

- High efficiency
- Long operating life
- Low Noise
- Variable High speed ranges[1]

The BLDCs main disadvantage is its cost.

1.3 A brief review on control of the BLDC motor

For sensored BLDCs, Hall Effect devices are present in the stator to detect the rotor position. These sensors face the magnets perpendicularly and can distinguish if the North or South Pole is in front of it.

As mentioned earlier, using Hall Sensors in the BLDC can lead to an increase of the overall price of the motor due to an increase in the wiring. Moreover, there are situations where sensors cannot be used in an application such as submersible pumps. In such

applications, the sensorless BLDC control is used. Various control system techniques/ algorithms such as Direct Back EMF zero crossing, Indirect Back EMF Integration and Field Oriented Control (FOC) are used to operate the motor.

1.4 Problem Statement

Conventional DC motors are being replaced by BLDCs due to their high efficiency and low noise features which are more desirable for consumers. Applications are broken down into three different types which were discussed in section 1.2. Due to a major disadvantage associated with BLDCs regarding the variable speed operation, various studies are being done in order to operate the BLDCs with constant speed. This allows BLDCs to be used in applications that require constant speed with varying load.

Since BLDCs are more expensive than the conventional DC motors, various approaches have been taken to reduce the cost of the BLDCs. BLDCs with Hall Effect sensors are being replaced with sensorless control techniques. These sensorless techniques require a complex algorithm which are not always easy to implement.

1.5 Thesis Organization

The rest of the thesis is organized as follows:

Chapter 2- Describes the construction, working principles and architecture of a BLDC control system.

Chapter 3- Explains different types of control techniques used for BLDC control. The techniques explained in this chapter are Hall Effect sensor, Direct Back EMF zero crossing control, Indirect Back EMF and Field Oriented Control.

Chapter 4- The speed vs. torque relationship of a separately excited DC motor and a BLDC are explained and compared in this chapter. A PI feedback control is introduced in this chapter for controlling the speed vs. torque of a BLDC.

Chapter 5- Compares the experimental results of the different BLDC control methods, without and with PI feedback control.

Chapter 6- Conclusion and Future work are discussed in this chapter.

Chapter 2

Overview of BLDC Design and Control

2.1 BLDC Motor Construction

BLDC motors share some similarities with induction motors and brushed DC motors in terms of construction and working principles. Just like all motors, BLDCs have two important parts: the rotor (rotating part) and the stator (stationary part).

The stator magnetic circuit is constructed using steel laminations. Steel laminations in the stator can be either slotted (inner rotor design) or slotless (outer rotor design) [14] as shown in Figure 2-1. The phase windings are wrapped around the stator, and they can be arranged in two patterns – star (Y) or delta (Δ). The Y pattern gives high torque at low RPM and the Δ pattern is used in order to give low torque at low RPM[2].

The rotor of a BLDC is constructed with permanent magnets, and it can consist of various numbers of poles based on the application. Increasing the number of poles gives higher torque but at the cost of reducing the maximum speed. There are two types of BLDC motor designs: Inner and Outer rotor design. In an outer rotor design, the windings are located in the center of the motor and the rotor magnets surround the stator windings. However, the rotor magnets act as an insulator, thereby reducing the rate of heat dissipation

from the motor. Due to the location of the stator windings, outer rotor designs typically operate at lower duty cycles or at a lower rated current. The primary advantage of an outer rotor BLDC motor is lower cogging torque[2].

In the inner rotor design, the rotor magnets are surrounded by the stator windings which are affixed to the motor's housing. The primary advantage of an inner rotor construction is its ability to dissipate heat. A motor's ability to dissipate heat also increases its ability to produce torque. For this reason, majority of BLDC motors use an inner rotor design. Another advantage of an inner rotor design is lower rotor inertia[2] which is a factor for speed control.

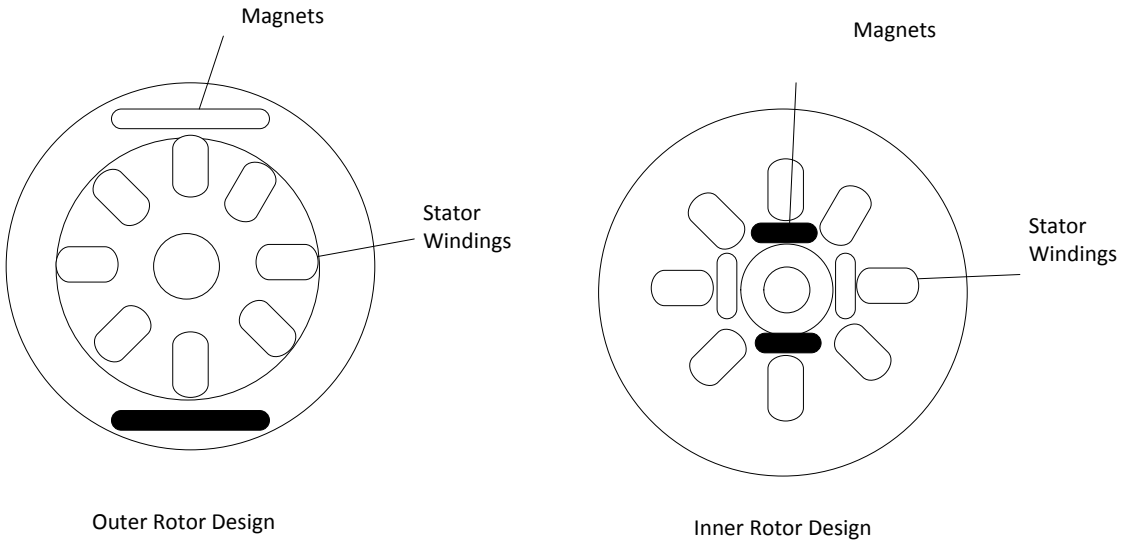

Figure 2-1: Outer and Inner Rotor Design of BLDCs [19]

The BLDC also is referred to as an electronically commuted motor since there are no brushes on the rotor, and commutation is performed electronically at certain rotor positions. Magnetization of the permanent magnets and their displacement on the rotor are

chosen in such a way that the Back- EMF (the voltage induced into the stator winding due to rotor movement) shape is trapezoidal. This allows a rectangular- shaped 3-phase voltage system to be used to create a rotational field with low torque ripple. This differs from Permanent Magnet Synchronous Motor (PMSM) which uses a sinusoidal 3-phase voltage to create a rotational field. PMSMs also have low torque ripple.

The BLDC is usually controlled using a three phase power semiconductor bridge. Control of the bridge requires the rotor position which is obtained using a sensor or a sensorless control technique.

2.2. Architecture of the BLDC system

The block diagram of a BLDC motor control system is shown in Figure 2-2. The four main parts of the BLDC control system are the power converter, controller, sensors and motor. The power converter is a three phase power semiconductor bridge shown in Figure 2-3. The main function of the power converter is to transform power from the DC source to AC so the motor can convert electrical energy to mechanical energy. The sensor is used to determine the rotor position, and it sends this information to the controller.

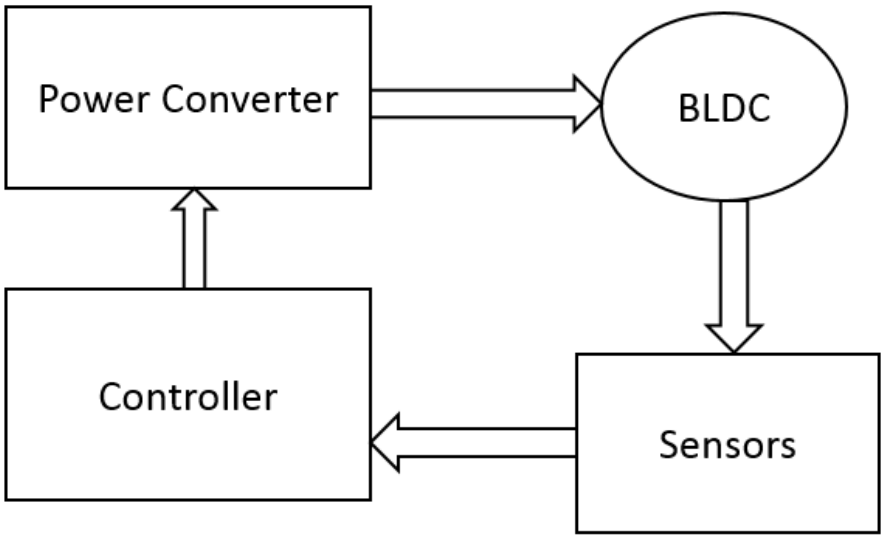

Figure 2-2: Block Diagram of BLDC Control [1]

The controller requires feedback information about the rotor position so it can generate a pulse width modulation (PWM) duty cycle to power the phases of the semiconductor bridge. The controller uses a PWM modulator to generate signals which drive the power converter. The internal block diagram of the power converter and controller is shown in Figure 2-3.

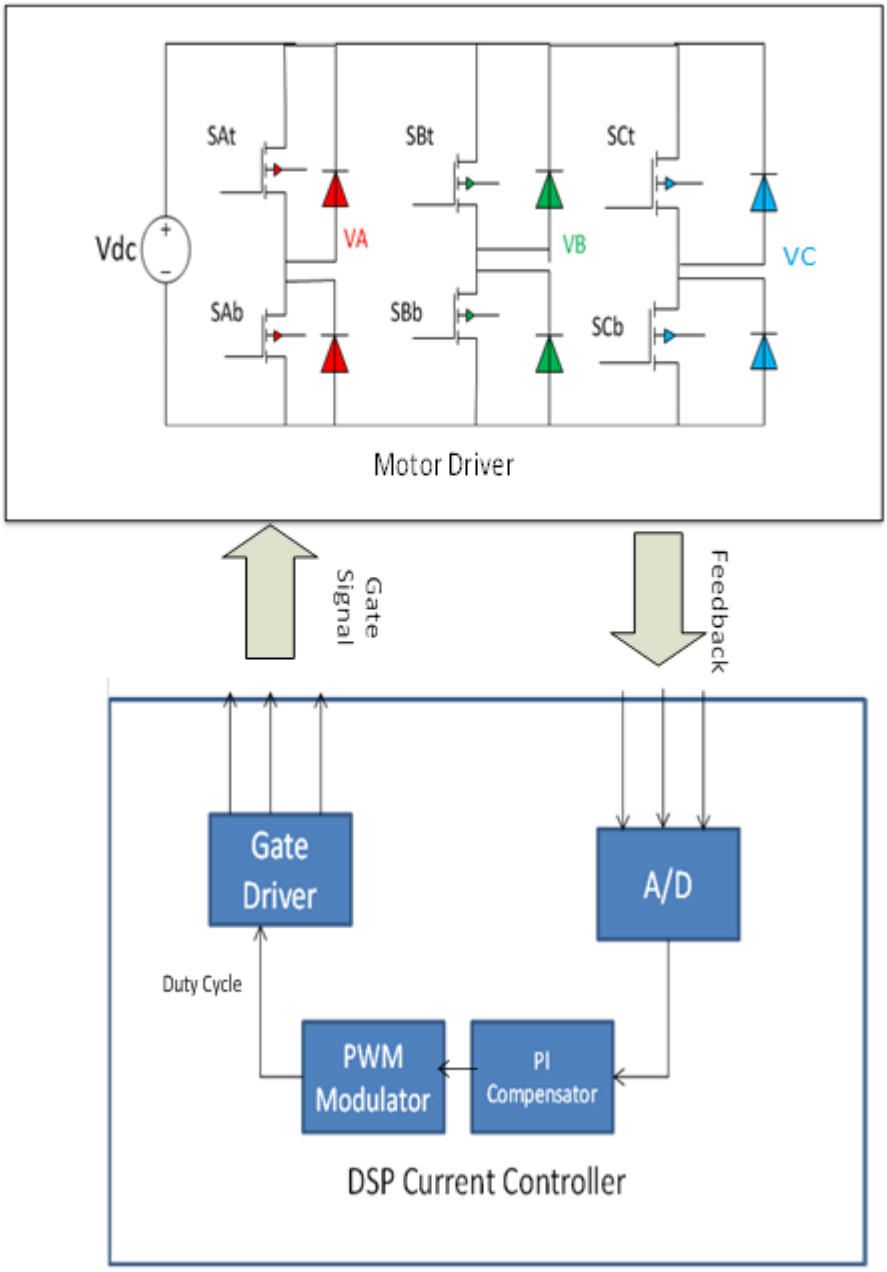

Figure 2-3: Internal Block Diagram of the Power Converter and Controller [1]

The speed of a BLDC is directly proportional to the voltage, and the applied voltage is increased or decreased accordingly. In a PWM controller, the PWM duty cycle controls

the voltage [3]. As voltage is applied, a current flow through the windings of the motor and this current provides torque to spin the motor. The motor can spin either in clockwise or counterclockwise direction by applying positive or negative voltage.

Chapter 3

Control Theory

The chapter focuses on various sensorless and sensored commutation techniques required to drive the motor. Earlier BLDC controllers required the use of Hall Effect devices to sense the angular position of the rotor magnets. Sensorless control techniques are introduced to reduce the cost of the system. Some of the sensorless control techniques explained in this chapter use Back- EMF and current sensing, which provide enough information to determine the position of the rotor and, therefore, to operate the motor with synchronous phase currents. Various concepts are discussed and advantages and disadvantages are included.

The techniques discussed in this chapter are:

a. Hall Sensors – Sensored Technique
b. Back- EMF Method:
    i. Direct Back EMF zero crossing /Terminal Voltage Sensing/ Trapezoidal Control– Sensorless Control Technique
    ii. Indirect Back EMF- Sensorless Technique
c. Field Oriented Control – Sensorless Control Technique

3.1 Hall Effect sensors

Hall Effect sensors are based on Hall Effect theory, which states that an electric current in a conductor produces magnetic field that exerts a transverse force on the moving charge carriers, and this tends to push them to one side of the conductor. A build- up of charge at the sides of the conductor will balance this magnetic influence, producing a measurable transverse voltage which is called the Hall Effect. This theory was discovered by Edwin Hall in 1879[2].

BLDC motor commutation is controlled electronically. The motor is rotated by energizing the stator windings in a particular sequence, and in order to do this it is important to know the rotor position. Rotor position is sensed using Hall Effect sensors which are embedded in the stator. The position of the Hall Effect sensor is shown in Figure 3-1 below.

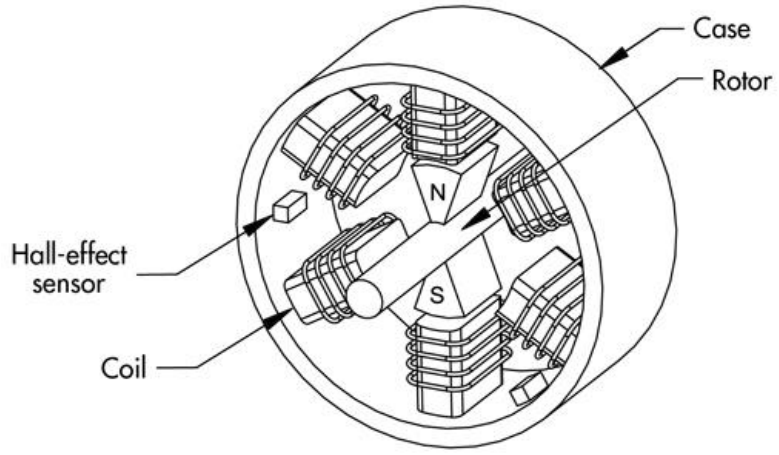

Figure 3-1: Position of Hall Effect Sensors[4]

As the rotor magnetic poles pass the sensor, the sensor changes state at the same angular position each time a magnet passes by. Therefore, whenever the rotor magnetic

poles pass near the Hall sensor, the sensor sends a high or a low signal for the North or South pole to the controller. Based on these combinations of sensor signals, the exact sequence for commutation can be determined.

Below are some of the advantages of a Hall Effect design:

- Hall Effect sensors provide a faster response time to a change in the magnetic field; therefore they provide greater efficiency in commutating a BLDC motor.
- Due to their accuracy they provide constant torque.
- They can provide high sensitivity and stability over temperature by using a technique called chopper stabilization[5][9].

The major disadvantage to a sensored technique is the cost due to the increase in the hardware and wiring.

3.2 Direct Back- EMF Zero Crossing Technique (Terminal Voltage Sensing/ Trapezoidal Control)

During the operation of a three- phase BLDC motor, two of the three phases are conducting at a time. The Back- EMF of the non- conducting phase is proportional to the speed, and the speed is proportional to the applied voltage as shown in Figure 3-2. The Back- EMF is zero at standstill and rises as the speed increases.

The zero crossing approach detects the instant at which the Back- EMF of the non-conducting phase crosses zero. This zero crossing triggers a timer, which may be as simple as a RC time constant. The next power stage commutation occurs at the end to this timing interval [6][9].

For proper operation of a BLDC motor, the phase current and the Back- EMF of the motor should be aligned in order to produce a constant torque[6][9]. Therefore, the current commutation point is estimated using the zero crossing point of the Back-EMF and a 30 degree phase shift [7][9].This is illustrated in the Figure 3- 2.

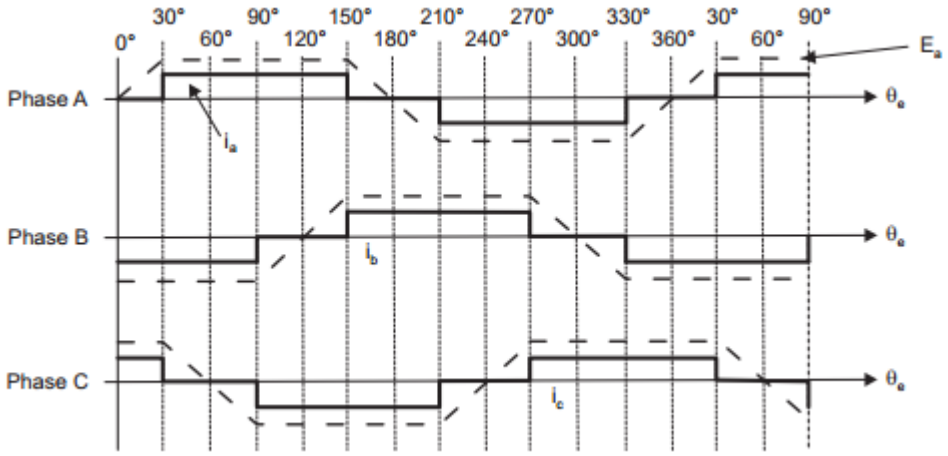

Figure 3-2: Alignment of Phase Back EMF and Current [9]

The conducting interval for each phase is 120 electrical degrees, and only two phases conduct current at any time. The third phase is floating or non-conducting. Figure 3-2 shows the alignment of the phase current and Back-EMF which is necessary to generate maximum torque. Therefore, the inverter should be commutated every 30^0 after detecting the zero crossing of the non-conducting phase[6].

The delay of 30 electrical degrees from the zero crossing instant is shown in the Figure 3-2, and this delay is not affected by any speed changes[8]. To detect the zero crossing point, the Back- EMF of the non- conducting phase needs to be monitored, and

the measurement should be low pass filtered to eliminate EMI caused by inverter switching [9].

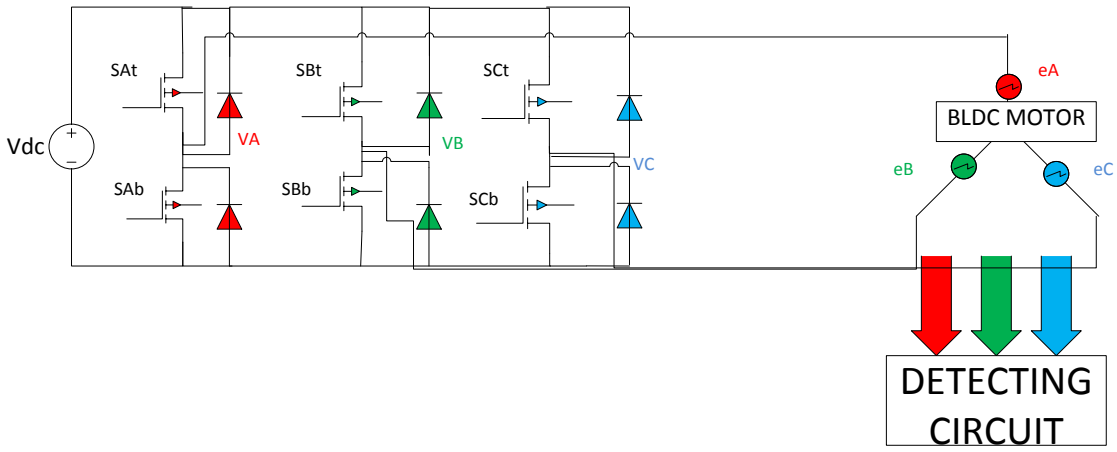

Figure 3-3: Three Phase Inverter and BLDC [9]

The terminal voltage of the non-conducting/floating phase is given by equation (3.1)[10]

$$V_c = e_c + V_N = e_c + (V_{CE} - V_F)/2 - (e_A + e_A)/2 \quad (3.1)$$

Where e_c-is the Back- EMF of the open phase (C), V_N is the potential of the 3- Phase motor neutral point, and V_{CE}andV_F are the forward voltage drops of the transistors and diodes, respectively [9].

Since the Back- EMF of the two conducting phases (A and B) have the same amplitude but opposite signs, the terminal voltage of the non-conducting phase/floating phase is given by equation (3.2):

$$V_c = e_c + V_N = e_c + (V_{CE} - V_F)/2 = e_c + (V_B + V_A)/2 \quad (3.2)$$

Where,

$V_{CE} = V_B$ (Collector emitter voltage of transistor S_{Bb})

$$-V_F = V_A$$

Since the zero-crossing point detection is done at the end of the pulse width modulation (PWM) on- state and only the high side of the inverter is chopped, V_{CE} is similar for theS_{At}andS_{Bb} transistors (Fig 3-3), and the detection formula can be represented by the following equation [9],

$$V_C = e_c + V_N = e_c + (V_{CE}^{B-} + V_{D_C} - (V_{CE}^{A+})/2 \cong e_C + (V_{DC})/2 \quad (3.3)$$

Therefore, the zero crossing occurs when the voltage of the floating phase reaches one half of the DC rail voltage[6].This zero crossing point is detected at the end of the PWM period.

The main advantage of using the Back- EMF sensing technique is the simplicity of this control algorithm compared to other sensorless techniques. This technique is considered to be the simplest method of those analyzed in this chapter.

However, the zero crossing method tends to be noise sensitive in detecting the zero crossing, and this tends to degrade performance over wide speed ranges. The inability to obtain a switching pattern at low speeds due to low Back- EMF is another drawback of this technique[11].

3.3 Indirect Back EMF Integration Technique

Since filtering introduces a commutation delay at high speed and low Back- EMF causes a reduction in signal sensitivity at low speed, this causes the speed range to be reduced in the direct Back- EMF zero crossing detection method. In order to overcome this problem, the Indirect Back- EMF Integration Technique is used to reduce switching noise.

This technique determines the commutation instant by integrating the back EMF of the open phase as shown in Figure 3-4 after the zero crossing point. A certain threshold value is set for different speeds. Once the integral value reaches the pre- defined threshold value, which corresponds to a commutation point, the phase current is commutated.

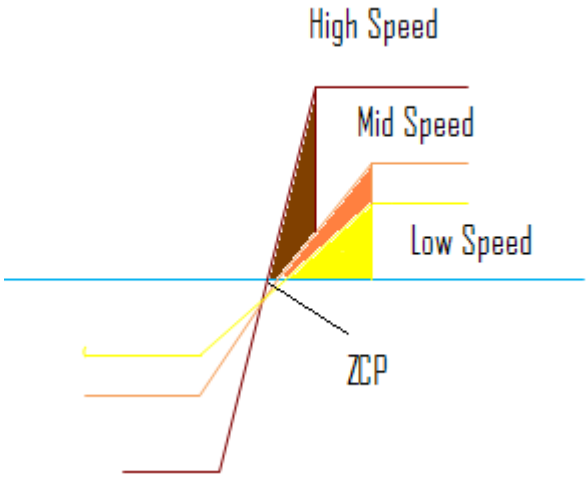

Figure 3-4: Integrated Area of the Back EMF for Different Speeds [9]

As shown in Figure 3-4 the highlighted areas in yellow, orange and brown represent low, mid and high speed, respectively. The highlighted areas presented in Figure 3-4 have the same area for different speeds. Each of these speeds has its own threshold voltage. Once the integrated value reaches the threshold voltage, a reset signal is asserted to zero the integrator output. The reset signal is active until the residual current in the open phase has passed a zero- crossing[12].

3.4 Field Oriented Control

As mentioned in the introduction, permanent magnet motors, including the BLDC and the Permanent Magnet Synchronous Motor (PMSM), have a wound stator, a permanent magnet rotor and a method to sense the rotor position which can be achieved internally or by an external device. The rotor position is necessary for the motor's operation. Similarly to the direct and indirect back EMF techniques, Field Oriented Control (FOC) is another control technique used to sense the rotor position without the help of sensors such as Hall Effect devices. FOC uses a different approach than the Back. EMF and is considered to be more effective and efficient when compared to other sensorless techniques. FOC also provides better performance over the torque range than the Back EMF methods[13].

FOC uses the mathematical processing power of microcontrollers and advanced control strategies to decouple the torque and magnetizing flux and provide a high dynamic performance drive system. This approach allows the BLDC to be an independent torque controller and field controller, as would be the case with a separately. excited DC motor[13].

To decouple the torque and the magnetizing flux component of stator current, it is necessary to use several mathematical transforms which are calculated by the microcontroller.

The torque produced in the synchronous machine is proportional to the vector cross product of the stator and rotor magnetic field, illustrated in equation (3.4)[13].

$$\tau = \vec{B}_{stator} \times \vec{B}_{rotor} \tag{3.4}$$

Where

τ – The torque, (N.m)

$\vec{B}_{stator}$ – Magnetic field of the stator, (Teslas)

$\vec{B}_{rotor}$- Magnetic field of the rotor, (Teslas).

This expression states that the maximum torque is achieved when the stator and rotor magnetic fields are orthogonal (90^0) to each other as shown in the Figure 3-5.

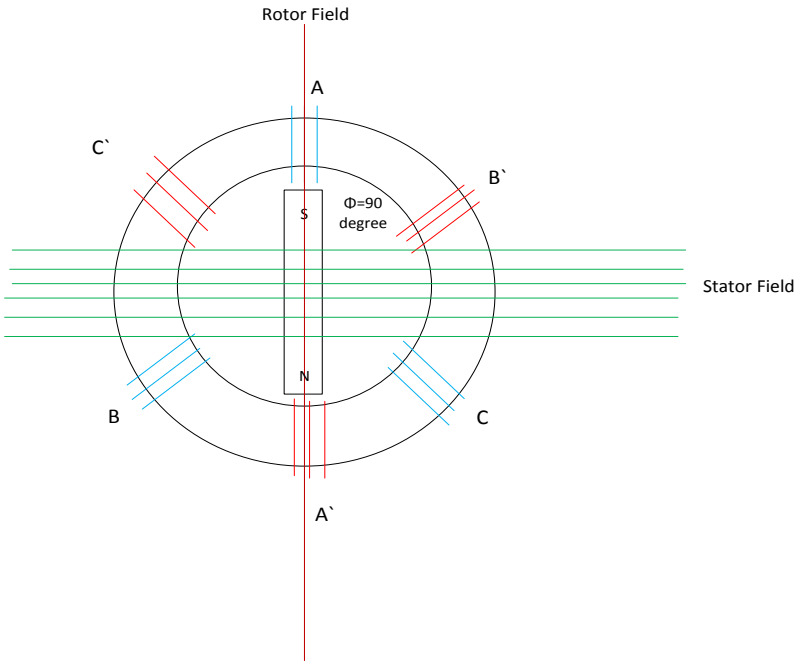

Figure 3-5: Rotor and Stator 90 Degree Position in the BLDC [13]

In brief, the FOC technique goal is to maintain the rotor and stator flux in quadrature by having the stator and rotor flux orthogonal to each other[13]. This control method is computationally intensive.

3.3.1 Rotating Reference Frame

In FOC, the rotor position is estimated by mapping the motor current into a rotating frame. The rotating frame constitutes of two axes – direct (*d*) and quadrature (*q*). The *d* axis is defined to be on the magnetic axis passing through the center of a set of permanent magnets on the rotor. The *q* axis is located orthogonally to the *d* axis. This is shown in the Figure 3-6.

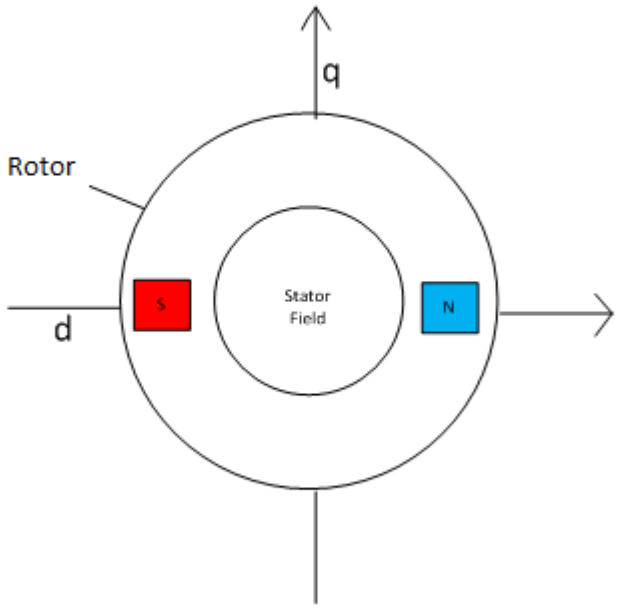

Figure 3-6: Rotating Frame Representation of the *d* and *q* Axes [13]

In order to find the rotor position, FOC needs two constants as input references: the torque component (aligned with the *q* co- ordinate) and the flux component (aligned with *d* co- ordinate)[13].

3.3.2 Space Vector Definition and Projection

The stator currents of two phases are known and third phase is determined using Kirchoff's current law [14]. The current from the three phases are transformed into a time invariant two coordinate system. This is achieved by the following two steps:

- $(a,b,c) \rightarrow (\alpha,\beta)$ Projection (Clarke Transformation)
- $(\alpha,\beta) \rightarrow (d,q)$ Projection (Park Transformation)

3.3.2.1 The $(a,b,c) \rightarrow (\alpha,\beta)$ Projection (Clarke Transformation)

The Clarke transformation transforms the current in the three phases into a 2- axis co- ordinate system ($i_{s\alpha}$and $i_{s\beta}$) as shown in Figure 3-7

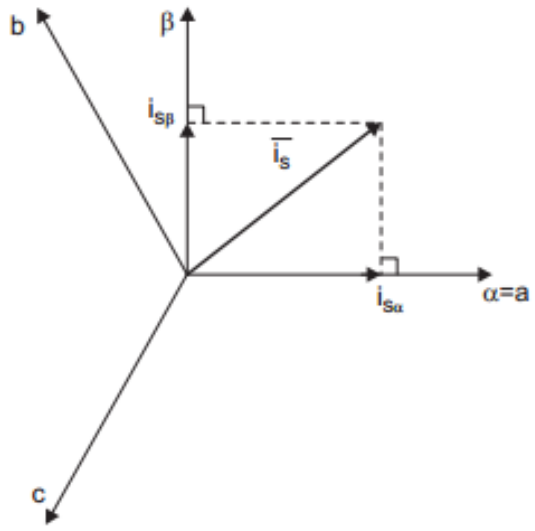

Figure 3-7: Two Axis Coordinate System [13]

3.3.2.2 The (α,β) → (d,q) Projection (Park Transformation)

The final stage in FOC is the Park Transformation which transforms the two phase (α,β) system obtained from the Clarke Transformation to the d, q rotating reference frame to locate the position of the rotor. The d and q components are determined through the rotor flux position θ. The block diagram of the FOC technique is shown in Figure 3-8

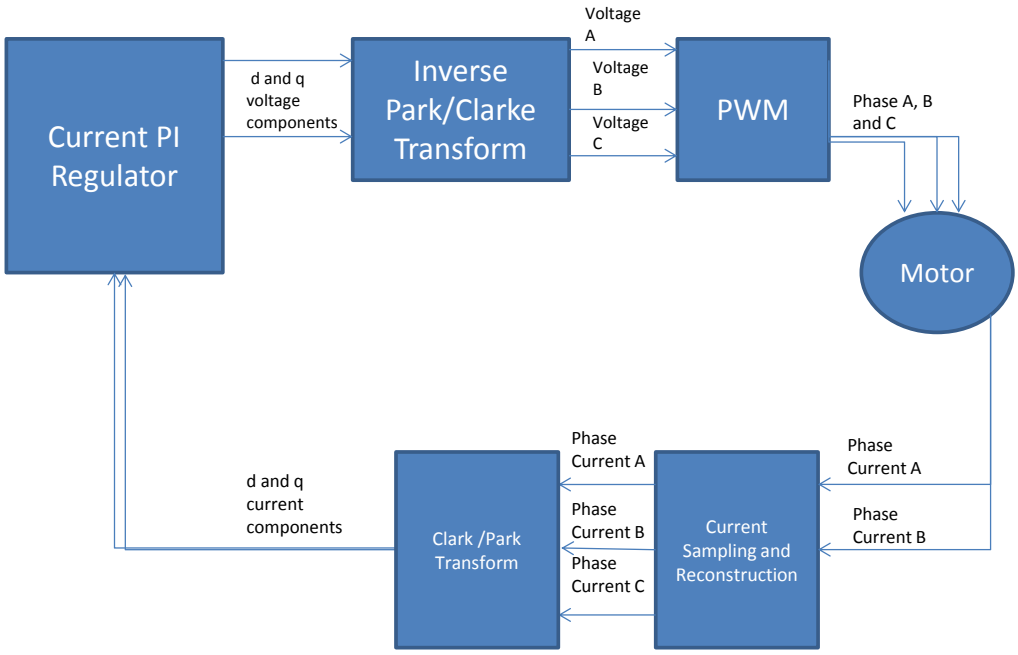

Figure 3-8: Internal Block Diagram of FOC [13]

3.3.3 Rotor flux position

The measure of the rotor flux position is a key component in finding the rotor position using the FOC algorithm. In a synchronous machine, the rotor speed is equal to the rotor flux speed. Rotor flux is directly measured by a position sensor or by Back- EMF.

In an asynchronous machine the rotor speed is not equal to the rotor flux speed. This needs to be calculated by a particular method using the *d, q* reference frame as explained in the above section.

The FOC provides various advantages which include 100% torque at start up, and quick calculation of rotor position that is required for commutation. It works well for various motors such as induction, PMSM or BLDC.

One of the main disadvantages of the FOC technique is the complexity of the algorithm which has to be programmed in a microcontroller to find the rotor position for commutation.

Chapter 4

Speed- Torque Relationship of the BLDC

BLDCs have been introduced to replace DC motors to provide more efficiency and lower cost. The speed vs. torque relationship for the BLDC is linear, but speed decreases as the load torque increases. In comparison, the speed of separately excited DC motor decreases only gradually as load torque increases.

A velocity control loop is used in some BLDC controllers to provide constant speed over the torque range. This chapter has two objectives: first is to understand the speed vs. torque characteristics of BLDCs and second, to understand the principles and design of a velocity control loop using a proportional integral (PI) controller.

4.1 Torque- Speed characteristics

For the study of electric motors, it is important to understand the term torque. By definition, torque is the product of force and radius to rotate an object about its axis [15]

$$Torque(N,m) = Force(N) X\ Radius\ (m) \tag{4.1}$$

Therefore for a BLDC, torque can be increased by either increasing the force or the radius. The force can be increased by using stronger magnets or increasing the currents in

the phases. A typical speed- torque characteristic graph of a BLDC is shown in Figure 4-1.

.

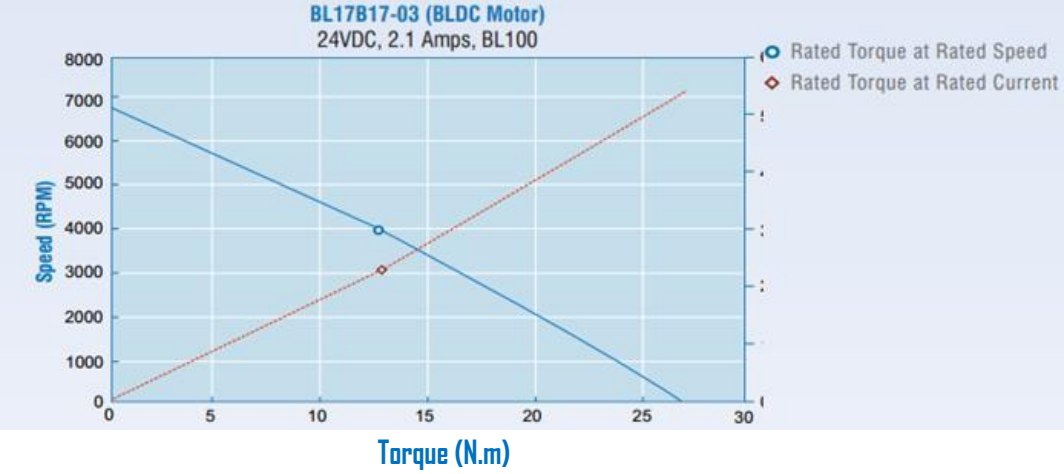

Figure 4-1: Speed vs. Torque of a BLDC [2]

The torque of a separately excited DC motor shown in Figure 4.2 is provided by equation (4.2)[16]

$$Torque = K_a \emptyset I_a \ (N.m) \tag{4.2}$$

Where:

K_a- Armature constant

$\emptyset$- Flux of the machine (Weber)

I_a- Armature current (Ampere)

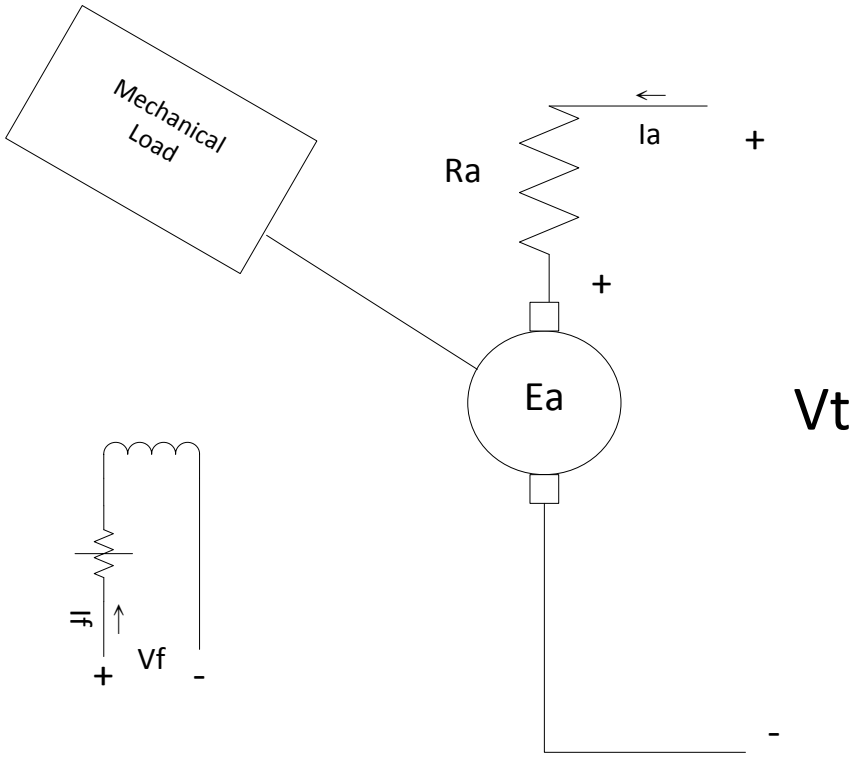

Figure 4-2: Separately Excited DC Motor [15]

The Back- EMF of a separately excited DC motor is [15]:

$$E_a = K_a \emptyset \, \omega_m = V_t - I_a R_a \tag{4.3}$$

Where,

E_a- Back- EMF (Volts)

ω_m - Speed (Radians/second)

V_t- Terminal voltage (Volts)

From Figure 4-2, Vf and If are the field voltage and field current respectively.

Figure 4-3: Speed vs. Torque of a Separately Excited DC Motor [15]

The speed- torque characteristic graph of a separately excited DC motor is shown in Figure 4-3. As shown in the figure, the speed drop over the torque range is very small, hence providing good speed regulation, unlike the BLDC. Speed in a DC machine increases as the terminal voltage increases.

By adding a velocity loop to a BLDC control system, speed can be held constant across varying torque. This velocity control loop uses a Proportional Integral (PI) Controller for speed regulation. A PI controller corrects the error between a measured process variable and desired set point by calculating and then outputting corrective action that can adjust the process accordingly [17]as shown in Figure 4-4.

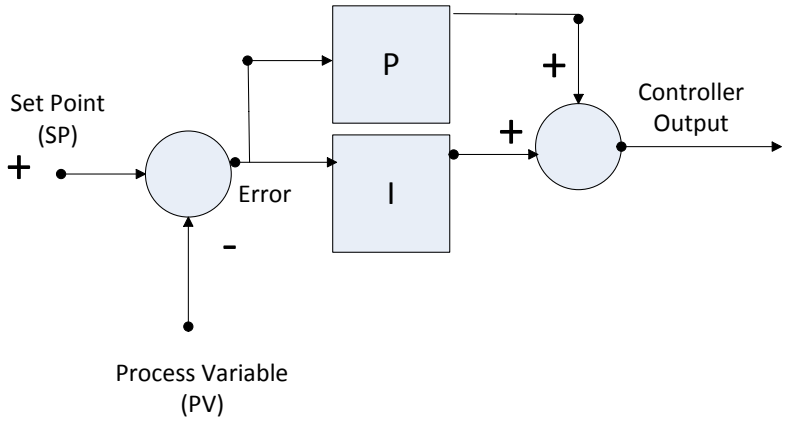

Figure 4-4: Block Diagram of a PI Controller [16]

The PI controller has two modes of control – Proportional (P) and Integral (I). For a given error signal changing over time in a control closed loop system, the proportional mode multiplies the error by the gain K_p. Therefore, if the error is large the proportional gain will produce a larger output and if the error is zero the proportional gain will produce a zero output. The integral mode continuously sums and multiples the error (changing over time) with the gainK_i. The integral mode is used to remove constant error. Therefore, no matter how small the constant error is, the summation of the error is going to be significant enough to adjust the controllers output [17]. The PI controller output is:

$$Output = Kp\ e(t) + Ki\ \int_0^t e(\tau)d\tau \tag{4.4}$$

Where:

Kp- Proportional gain

Ki- Integral gain

e- Error ($(Sp\ (Set\ Point) - Pv(Process\ Variable)$)

t- Time

4.2 Velocity Control Using a PI Controller in a BLDC Drive:

The speed is controlled using a velocity controller which is implemented using a conventional PI controller. The difference between the actual speed and the desired speed is fed as an input to the PI controller, and based on this difference, the PI controller controls the duty cycle of the PWM pulses to the 6 transistors in the inverter. This controls the voltage amplitude required to maintain the desired speed. This process is illustrated in the block diagram shown in Figure 4-5.

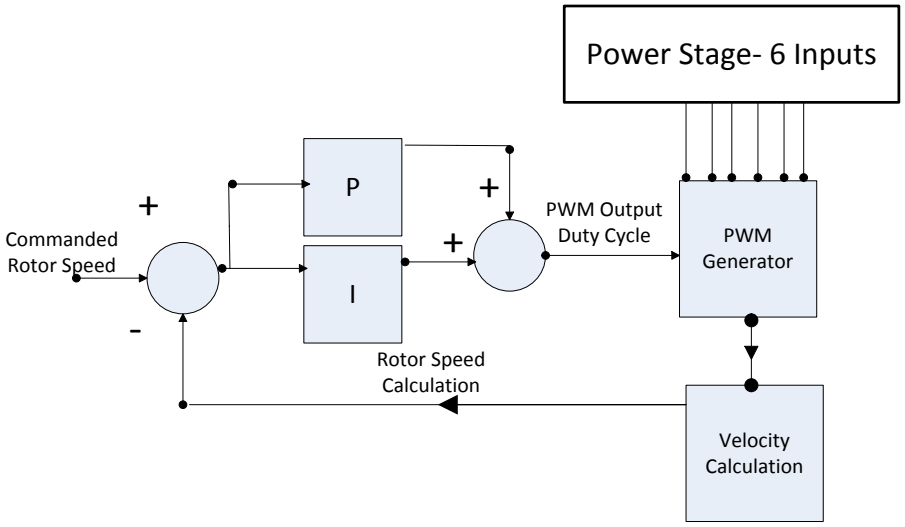

Figure 4-5: Block Diagram of a Velocity Control Loop for a BLDC with PI Control [17]

4.2.1 Tuning the K_p and K_i Gains:

Speed control depends on knowledge of the inertia of the load, mechanical linkages, and desired response [18]. Gains K_p and K_i need to be tuned accordingly to get a stable system. $K_p$and K_i are initialized using a "rule of thumb", which works well for most

motors[18]. The open loop transfer function of the system presented in equation (4.5) and (4.6) [18] is obtained from the closed loop velocity control system in Figure 4-6.

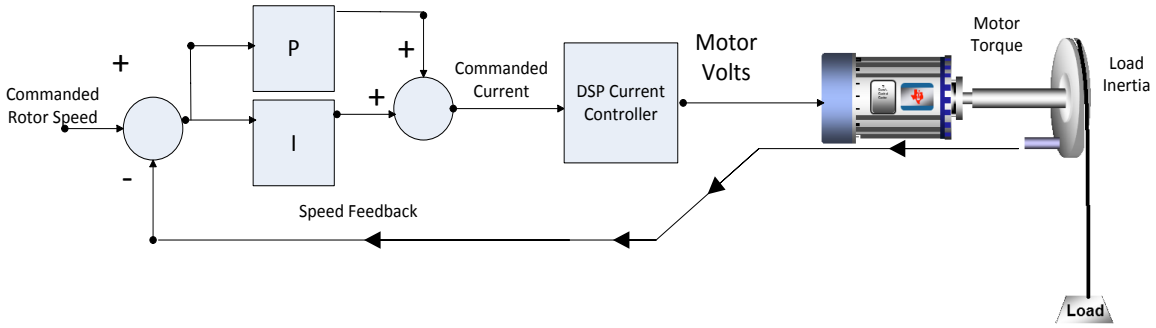

Figure 4-6: Closed Loop Velocity Control using PI for a BLDC [17]

$$G_{loop}(s) = PI(s)\ x\ K_{curr}\ x\ Mech(s) = K_i\left(\frac{1+\frac{Kp}{Ki}s}{s}\right)K_{curr}\ \left(\frac{K}{s}\right) \qquad (4.5)$$

$$G_{loop}(s) = \frac{KK_{curr}K_i}{s^2}\left(1+\frac{Kp}{Ki}s\right) \qquad (4.6)$$

Where,

K_{curr}- Gain of current controller

The closed loop transfer function$\left(\frac{G_{loop}(s)}{1+G_{loop}(s)}\right)$ of (4.6) is

$$G_{loop}(s) = \frac{KK_{curr}K_i\left(\frac{1+\frac{Kp}{Ki}s}{s}\right)}{s^2+KK_{curr}K_ps+KK_{curr}K_i} \qquad (4.7)$$

Stiffness is the property of a system that dictates how aggressively the system will reject disturbances [18]. The stiffness of the motor depends on K_i, and as we increase $K_i$the stiffness of the motor system increases. Similarly, gain K_p controls the damping of the system, which is a property that reduces or dissipates heat energy as rapidly as possible in

order to reduce oscillations and get a stable system [19]. By applying a load to this system, it was observed that by having a high K_i and low K_p the system had large oscillations and was unstable. Therefore, to achieve a stable system the gain $K_p$was increased.

The proper K_p and $K_i$can vary for different BLDCs. For a given test, the gains are set high which results in a stable system at higher speed, but once the speed is lowered, the system tends to be unstable. This is due to the duration of the commutation interval. When the motor is spinning at high speed, there are many commutation intervals per second, which means that the velocity feedback value is updated many times per second. However, when the motor is spinning at low speed, the commutation rate is low, which means the update rate for the velocity value is also low, and this causes a phase lag between the true velocity and the measured velocity. Since the velocity value is not updated frequently, the control becomes unstable.

Chapter 5

Experimental Results

5.1 Prony Brake Dynamometer

The speed vs. torque characteristics of two different BLDCs were measured using a Prony Brake Dynamometer, which is a simple type of dynamometer used to measure the torque. This device was invented by French Engineer Gaspard de Prony in 1821. A Prony brake consists of a leather strap wrapped around a pulley which is connected directly to the shaft of the motor as shown in Figure 5-1. Two spring scales are attached to both ends of the leather strap to measure the force on the pulley when the motor is running in either direction.

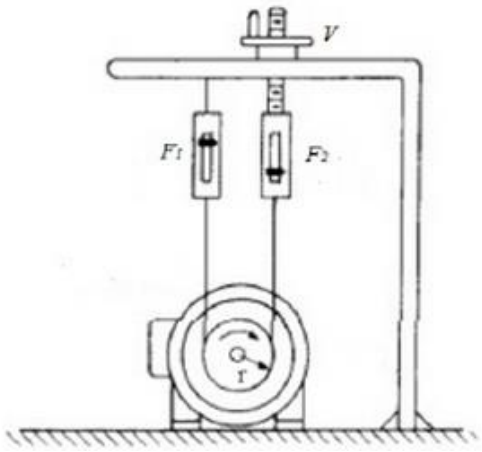

Figure 5-1: Prony Brake Dynamometer[20]

From Figure 5-1, F1 and F2 are the two force deflections on the spring scales. When the motor is spinning in clockwise direction there is deflection in spring F1 but not F2, and when the motor is spinning in counter clockwise there is deflection on spring F2 but not F1. The prony brake dynamometer setup in the lab is shown in Figure 5-2. The measured torque is given by (5.1)

$$Torque = F\ x\ r\ (lbs.ft) \tag{5.1}$$

Where,

F- Spring force (lbs.)

r- Radius (ft.)

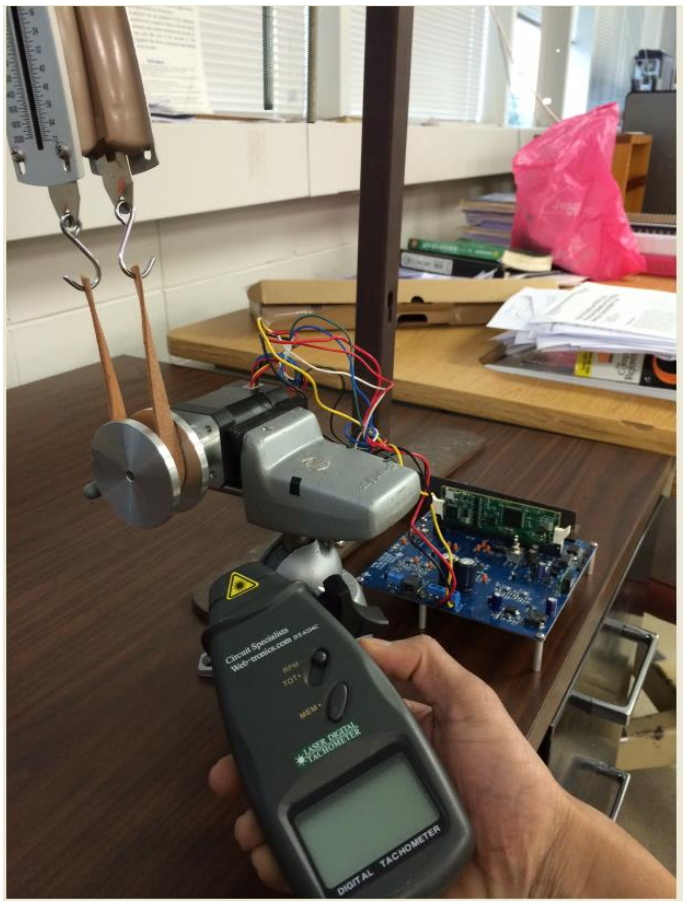

Figure 5- 2: Prony Brake Setup

5.2 Test Results of Speed vs. Torque for Different BLDC Control Techniques

To compare speed vs. torque characteristics for different control techniques, a BLDC kit from Texas Instruments (TI) – DRV8312- 69M and one from Freescale – 3Phase- LV kits were tested. These kits were operated using various control techniques such as Hall Effect sensors, Trapezoidal Back EMF (Direct Back EMF Zero Crossing),

Indirect Back EMF and Field Oriented Control (FOC). The speed vs. torque characteristics were measured using a strobe light and Prony brake dynamometer.

5.2.1 TI Kit- DRV8312- 69M

The DRV8312- 69M kit shown in Appendix A.1 uses a control technology developed by Texas Instruments called InstaSPIN. The InstaSPIN technology provides sensorless features such as InstaSPIN- FOC, InstaSPIN- BLDC and InstaSPIN- DRV8312 to control the motor using FOC, Indirect Back- EMF, and Trapezoidal control, respectively. This kit also provides sensored Trapezoidal Back- EMF control using Hall Effect sensors. The speeds vs. torque curves for different InstaSPIN technology are shown in Figure 5-3, 4, 5 and 6.

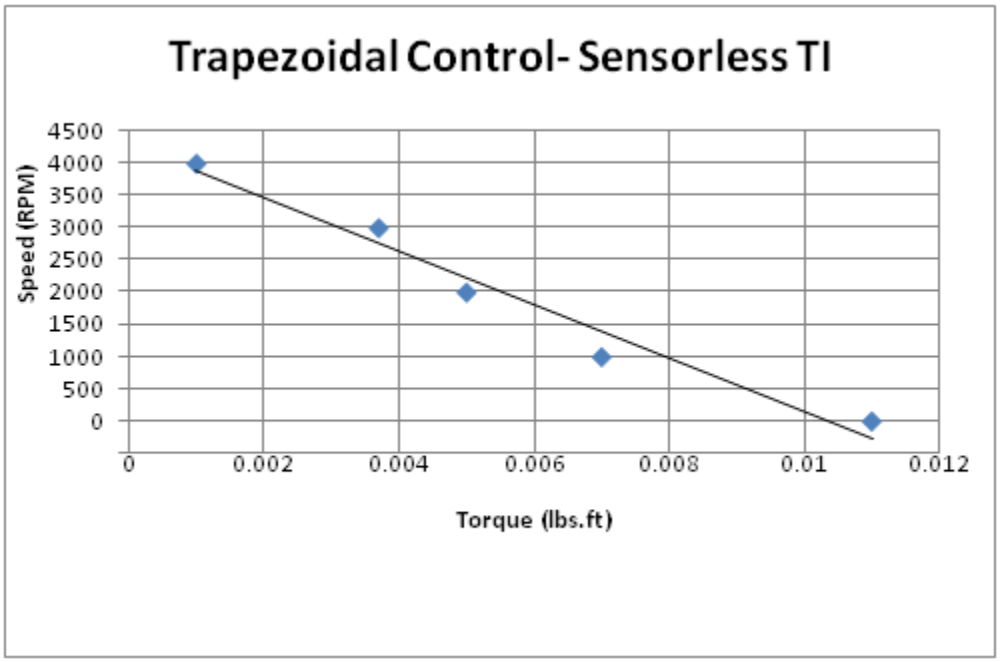

Figure 5-3: Speed vs. Torque of Trapezoidal BLDC Control by TI

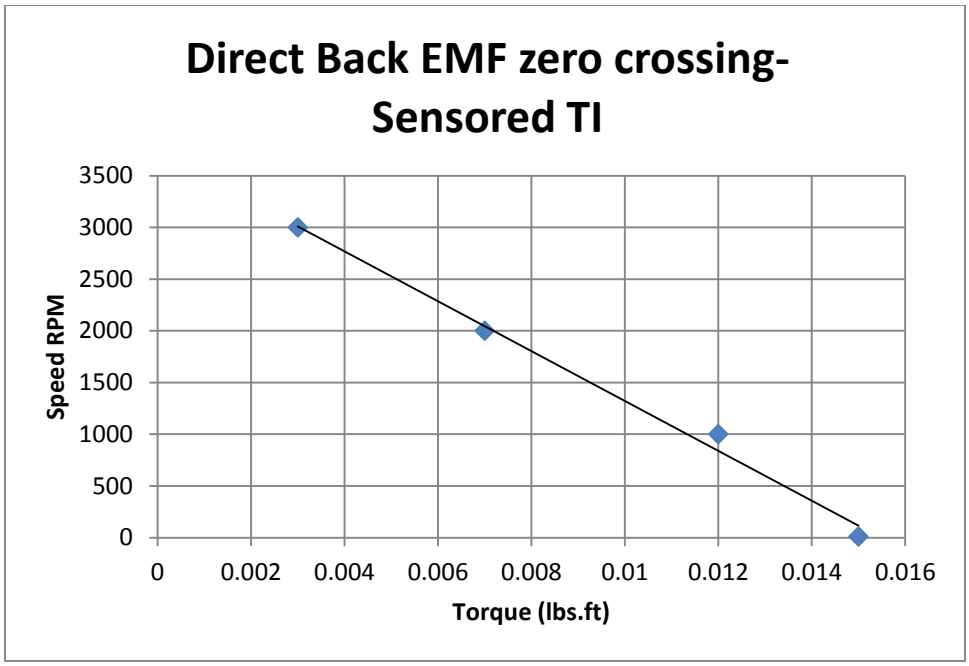

Figure 5-4: Speed vs. Torque of the Direct Back- EMF using Hall Effect Sensors by TI

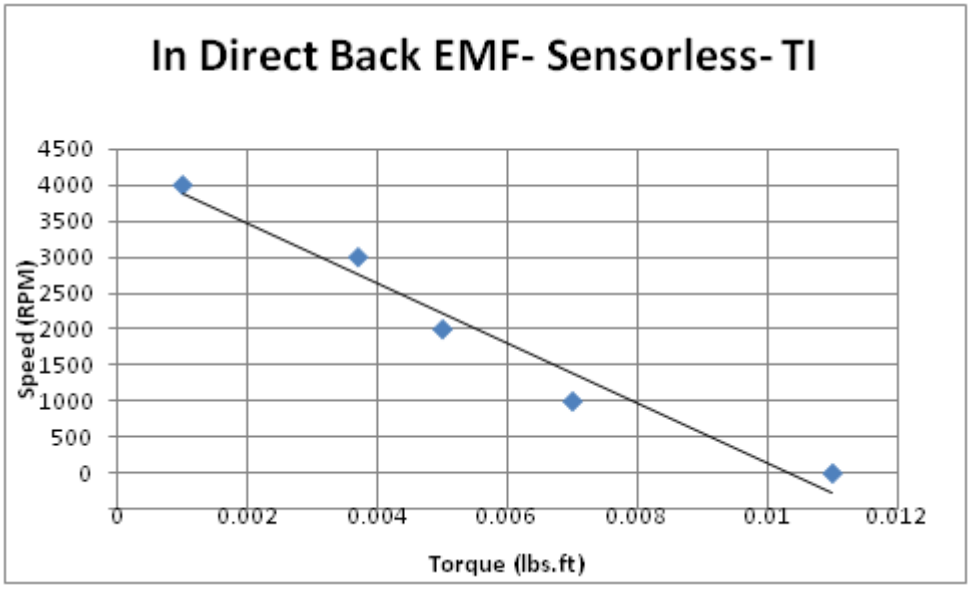

Figure 5-5: Speeds vs. Torque of Indirect Back EMF by TI

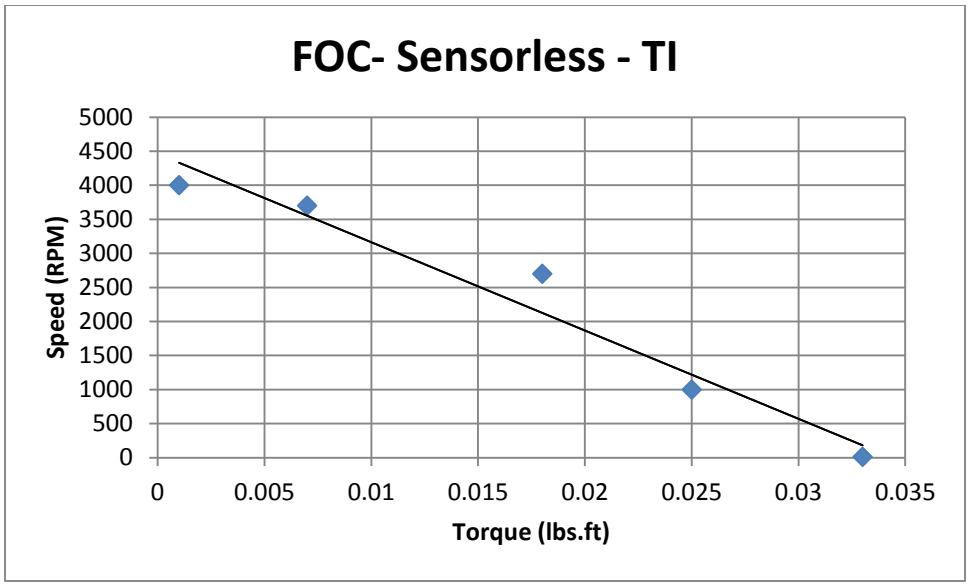

Figure 5-6: Speed vs. Torque of FOC by TI

5.2.2 Freescale- 3PhaseLV

The 3PhaseLV kit shown in Appendix A.2 comes with two microcontrollers: the MC56F8006 (32bit) and the MC9S08MP16 (8bit). The kit can operate the motor using the Indirect and Direct Back EMF techniques. The speed vs. torque curves are shown in the Figures 5-7 and 5-8.

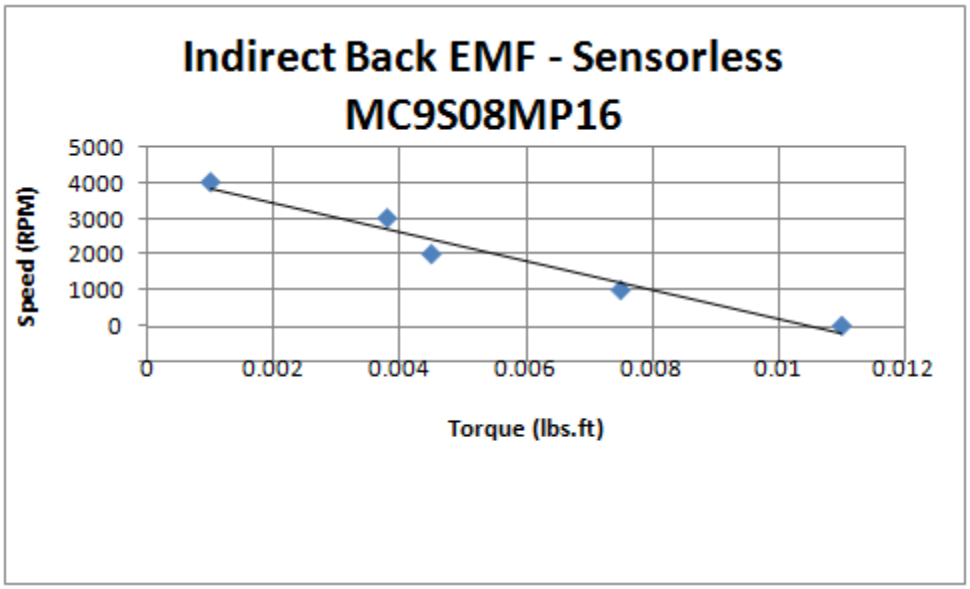

Figure 5-7: Speed vs. Torque of the Indirect Back EMF by Freescale

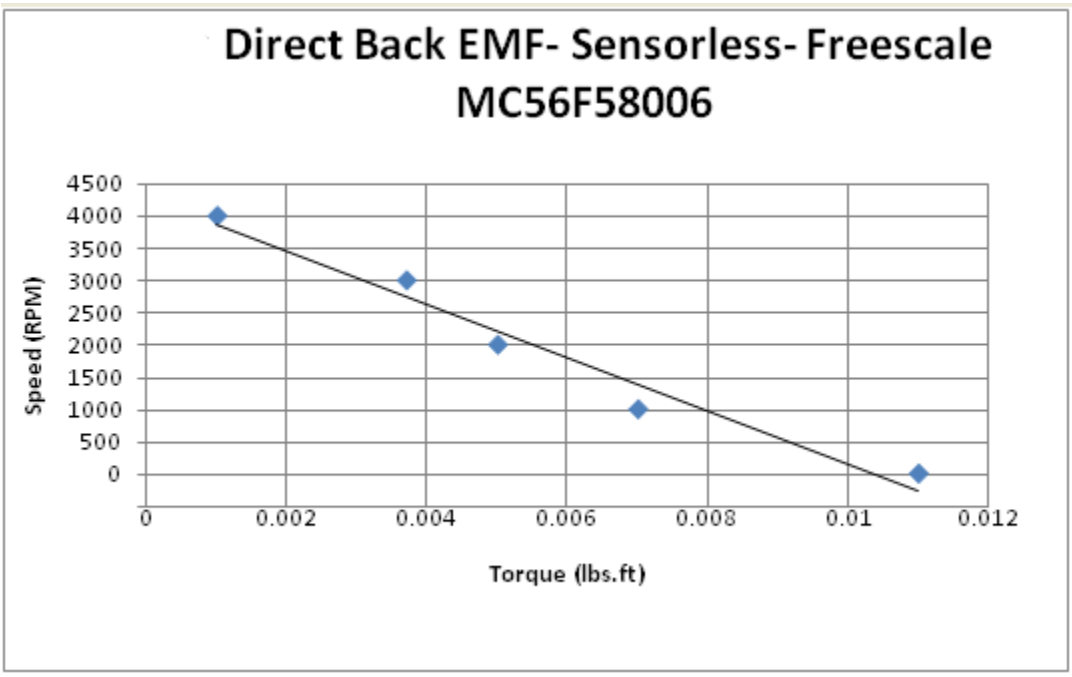

Figure 5-8: Speed vs. Torque of the Direct Back EMF by Freescale

As shown in Figures (5-3) to (5-8) the speed vs. torque curves for the sensored and sensorless control techniques share similar results. The speed varies linearly with respect to torque. The only difference between the graphs is the speed performance over load torque changes. The motor used in a Freescale kit is the 45ZWN24-40 (Rated Torque is 990 g.cm and Rated Power is 40 W) is a bigger motor than the motor used in the TI kit, the DT4260-24-055-04(Rated Torque is 640 g.cm and Rated Power is 26 W). FOC sensorless control by TI had the highest stall torque of all the methods including the Hall Effect sensor. This was very odd since Freescale had a bigger motor than TI.

In order to provide constant speed as torque varies, a velocity control loop has to be used for speed regulation. This is an important feature for the fixed speed applications.

The speed vs. torque characteristics of two velocity control systems using sensorless FOC and sensorless Indirect Back EMF control are shown in Figures 5-9 and 5-10.

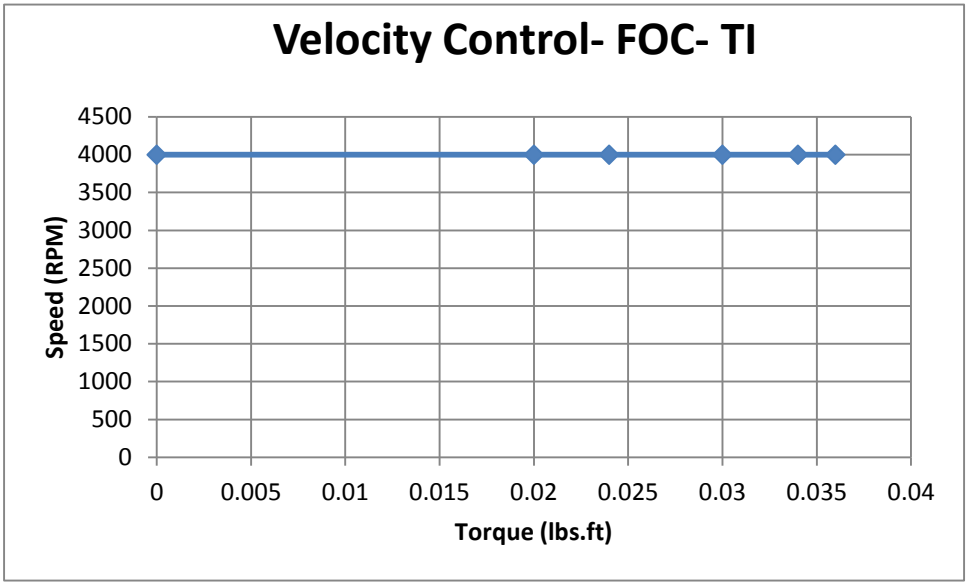

Figure 5-9: Speed vs. Torque of Velocity Control Loop Using FOC

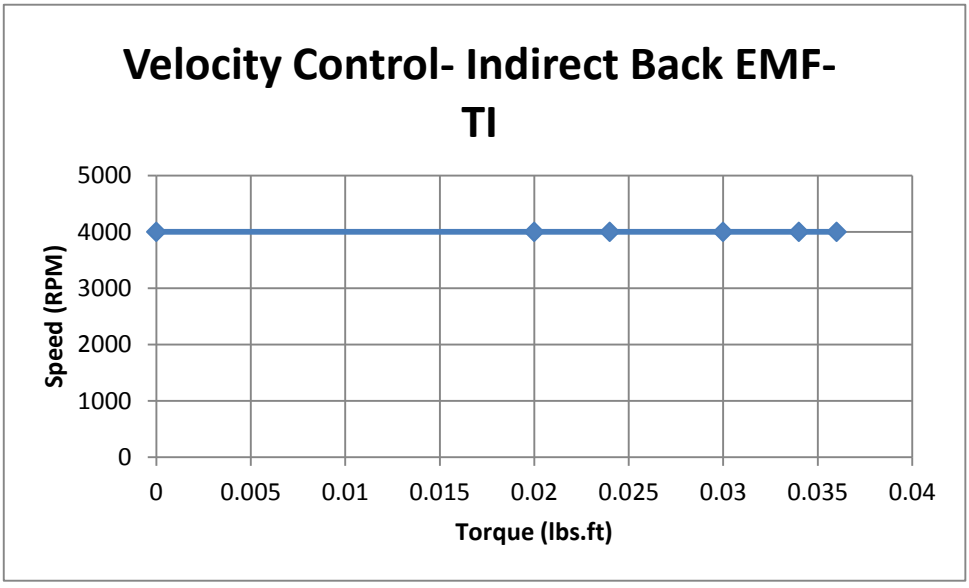

Figure 5-10: Speed vs. Torque of Velocity Control Loop Using Indirect BackEMF

Chapter 6

Conclusion and Future Work

6.1 Conclusion

BLDC are constantly replacing DC motors in various applications. These applications vary from fans, pumps, steering wheel and blowers to name a few. A typical BLDC behaves as a PM DC motor with linear speed vs. torque characteristics where the speed decreases as the load increases. Some applications, such as an automobile (Windscreen wiper), require the motor to have a fairly constant speed for different loads. DC motors such as shunt and compound work reasonably well in these applications, but a BLDC with a PI controller improves the performance. The speed vs. torque characteristics shown in Figure 5-9 and 10 show that the speed remains virtually constant across the torque range. These curves are more similar to a separately excited DC motor, but they are actually much better because of the feedback control.

Various sensorless control techniques are being introduced and researched in order to replace the use of sensor control techniques in a BLDC system. By doing this, the cost of the system can be reduced and BLDC can be more affordable. Techniques such as Direct Back EMF Zero Crossing, Indirect Back EMF Integration and Field Oriented Control

(FOC) were studied in this research. Direct Back EMF, Indirect Back EMF Integration and FOC share similar linear speed vs. torque relationship. This is illustrated in Figure 5-3, 5-4, 5-5, 5-6, 5-7 and 5-8. The only difference noticed in the speed vs. torque curve is the stall torque. The stall torque was different for all the techniques. FOC had the highest stall torque when compared to Direct Back Zero Crossing, Indirect Back EMF Integration and Hall Effect Sensor.

6.2 Future Work

To extend the research work presented in this thesis, future work may consider the following possibilities:

- Various other sensorless techniques apart from the techniques mentioned in this thesis report can be researched and applied to BLDCs.
- Various other techniques can be tested for speed vs. torque characteristics of BLDCs and can be compared to the speed vs. torque characteristics of a separately excited DC motor.
- Stall torque of various techniques can be measured and compared.
- A feedback control loop can be applied and speed vs. torque characteristics can be tested.

The three sensorless control techniques studied in this thesis are Direct Back EMF Zero Crossing, Indirect Back Integration and FOC. FOC is the most mathematically complex technique. The complexity of this technique is considered as a disadvantage, as this

techniques algorithm is difficult to comprehend. Future work in the study of simplifying the control algorithm of FOC is very important.

It is very important to tune Kp and Ki gain of the velocity control loop in order to get a stable system. In this study, the “rule of thumb was applied in tuning the gains Kp and Ki. However, to obtain more accurate values of Kp and Ki, future studies should consider applying more reliable tuning methods such as the Ziegler- Nicholas method [21].

References

[1] S. Rambabu, “MODELING AND CONTROL OF A BRUSHLESS DC MOTOR,”M.S. Thesis, National Institute of Technology, Rourkela, 2007.

[2] R. Gambhir and A. K. Jha, “Brushless DC Motor : Construction and Applications,” *Int. J. Eng. Sci.*, vol. 2, no. 5, pp. 72–77, 2013.

[3] L. Zhong, M. F. Rahman, W. Y. Hu, and K. Lim, "Analysis of direct torque control in permanent magnet synchronous motor drives," *IEEE Transactions on Power Electronics,* vol. 12, pp. 528-536, 1997.

[4] Galil, "Brushless Sine Drives- Application Note". [Online]. Available: http://www.galilmc.com/support/servotrends/st_04_11/sine-drive-setup.php

[5] B. Robert, H. H. Iu, and M. Feki, "Adaptive Time-Delayed Feedback For Chaos Control In A PWM Single Phase Inverter," *Journal of Circuits, Systems, and Computers,* vol. 13, pp. 519-534, 2004.

[6] Freescale, Appl. Note DRM117, pp 1- 27.

[7] G. Paranjothi and R. Manikandan, “Photovoltaic Based Brushless DC Motor Closed Loop Drive for Electric Vehicle,” *IJETEE*, vol. 10, no. 1, pp. 9–15, 2014.

[8] A. Dwivedi and A. N. Tiwari, “A Review : Speed Control of Brushless DC Motor,” *IJBSTR*, vol. 1, no. 6, pp. 14–19, 2013.

[9] T.-S. Kim, B.-G. Park, D.-M. Lee, J.-S. Ryu, and D.-S. Hyun, "A new approach to sensorless control method for brushless DC motors," *International Journal of Control, Automation, and Systems,* vol. 6, pp. 477-487, 2008.

[10] J. C. Gamazo-Real, E. Vázquez-Sánchez, and J. Gómez-Gil, “Position and speed control of brushless DC motors using sensorless techniques and application trends.,” *Sensors (Basel).*, vol. 10, no. 7, pp. 6901–47, Jan. 2010.

[11] Jianwen Shao, "Direct Back EMF Detection Method for Sensorless Brushless DC (BLDC) Motor Drives, M.S. Thesis, Virginia Polytechnic Institute and the State University.", Blacksburg, Virginia, 2003.

[12] Texas Instrument, Appl. Note SPRABN7, pp. 1-16

[13] Texas Instrument, Appl. Note SPRABQ9, pp 1-44

[14] Nilsson, James William, and Riedel, Susan, *Electric Circuits*. Vol. 8. Prentice Hall, 2009.

[15] P.C. Sen, *Principles of Electrical Machines and Power Electronics*, John Wiley & Sons, Inc., 1997.

[16] R. C. D. and R. H. Bishop, *Modern Control Systems*, 12th ed. Pearson, 2011.

[17] Texas Instrument, Appl. Note InstaSPIN Projects and Labs User's Guide, pp 81-86.

[18] Fabreeka,"Vibration and Shock Isolation". [Online]. Available: http://www.fabreeka.com/documents/file/papers/isolation_theory.pdf

[19] D. L. Gabriel and J. Meyer, "Brushless DC Motor Characterisation and Selection for a Fixed Wing UAV," *IEEE Africon 2011*, pp. 13–15, 2011.

[20] T. Wildi, *Electrical Machines , Drives and Power Systems, 6th Edition*, A. Wolf, Ed. United States of America: Prentice Hall, 2006.

[21] K. Åström and T. Hägglund, "Revisiting the Ziegler–Nichols step response method for PID control," *Journal of process control,* vol. 14, pp. 635-650, 2004.

Appendix A

BLDC KITS

The BLDC KITS used for test purposes were sponsored by Freescale and Texas Instruments. The two kits used are: 3Phase LV KIT (Freescale) and DRV8312- 69M (Texas Instruments).

A.1Texas Instruments- DRV8312- 69M KIT

Features:

- DRV8312 three phase inverter integrated power module base board supporting up to 50V and 3.5A.
- C2000 Piccolo TMS320F28069M Microcontroller
- 1 BLDC/BLAC NEMA17 55W Motor
- 24 V power supply
- USB Cable
- Operates on Trapezoidal Sensor and Sensorless Control, In- Direct Back EMF, and FOC

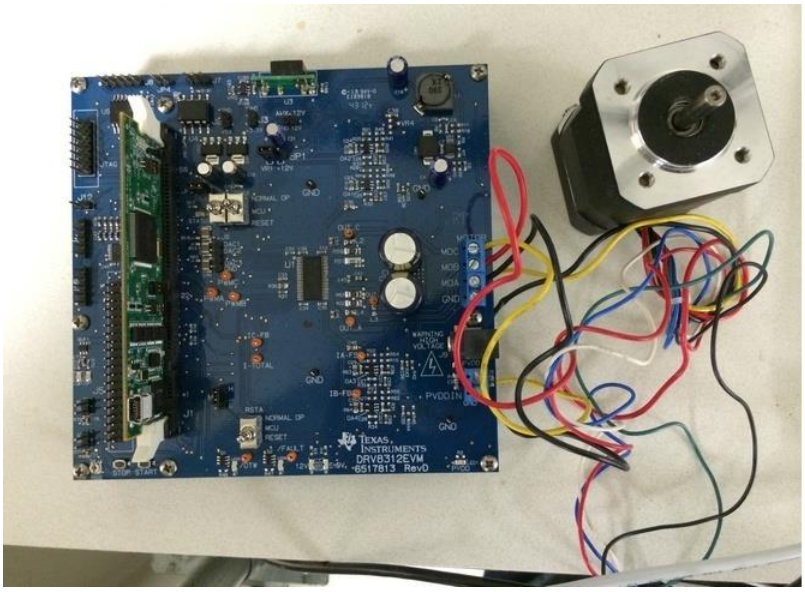

Figure A-1:DRV8312-69M kit by TI

Figure A-2:F2806x Microcontroller Card (32 bit)

A.2Freescale-3PhaseLV KIT

Features:

- Power supply 12–24 V DC
- 3-phase bridge inverter (MC33937)
- DCbus voltage sensing and 3 phase Back-EMF voltagesensing circuitry
- Encoder/hall sensor sensing circuitry
- USB interface
- Two microcontroller card. MC9S08MP16 and M656F8006
- 1 BLDC 45ZWN24.40

Figure A-3: 3 Phase LV kit by Freescale

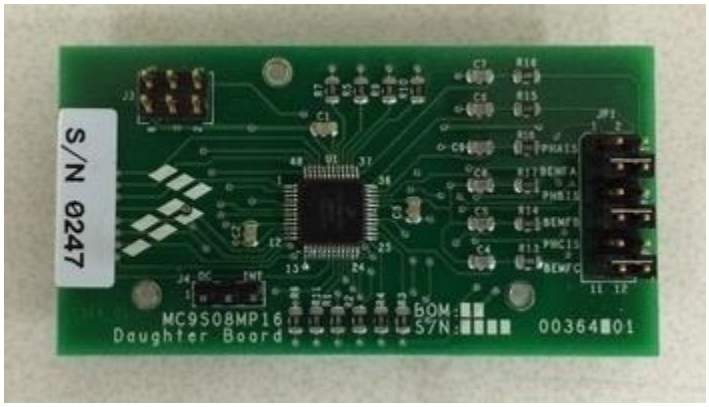

Figure A-4: Freescale- MC9S08MP16 Control Card (8 bit)

Figure A-5: Freescale- MC56F8006 Control Card (32 bit)